

THE USE OF ULTRASONIC TIME OF FLIGHT DIFFRACTION (TOFD) NDT AND FRACTURE MECHANICS FOR ACCURATE SERVICE LIFE PREDICTION OF A CARDEN SHAFT

R B Tait*, J Press** and Z McCann***

*Mechanical Engineering Department, University of Cape Town,

**Cape Residual Stress, P O Box 26891, Hout Bay, 7872

***Atomic Energy Authority, AEA Technology

ABSTRACT

For a large industrial shredder, the link between the 2.2MW motor and the shredder was facilitated by using a 2.5m Cardan shaft. Unexpected premature fracture of the shaft was the precursor to a weld repair, which also developed fatigue cracking within two months of operation. The shaft was weld repaired a second time, and a new shaft ordered from the US. However, in order to manage the operation of the plant safely, while awaiting the six-month delivery, it was appropriate to undertake a fracture mechanics based fatigue life prediction of the repaired shaft. To undertake such an assessment, reliable measures of flaw sizes were required.

This paper concerns this very fracture mechanics fatigue life analysis, which makes significant use of reliable flaw size estimates obtained using ultrasonic TOFD measurements. The flaw sizes determined using TOFD also correlated closely with the *actual* crack sizes revealed when the first repair was undertaken, further confirming the confidence in the TOFD methodology. Experimental strain gauge based stress analysis provided the actual cyclic load spectrum, and rigorous failure analysis of the first failure indicated that fatigue cracking initiated from the *inside* surface of the hollow shaft, thus necessitating ultrasonic, rather than other, NDT techniques. Accurate flaw sizing was necessary and TOFD, with an accuracy (in the field) of approximately $\pm 1.0\text{mm}$, was ideal. Plausible values of material parameters, flaw shapes and initial flaw sizes were used in the fatigue life prediction, which was itself updated and bench marked as the service life proceeded. The paper presents the findings of the TOFD dependent fracture mechanics based fatigue life prediction, and ultimately led to safe operation of the repaired Cardan shaft. There was no further breakdown up to the arrival of the replacement, despite the development of further cracking.

The case study presented in this paper is an ideal example of the mutual benefit of using high quality NDT, together with fracture mechanics techniques, for safe operation of a large and high valued engineering application.

1. INTRODUCTION AND BACKGROUND

While the topic “scrap metal” hardly brings to mind the concept of high tech equipment, it is nonetheless true that, in certain circumstances, some of the heavy plant and equipment used to process such recycled material can indeed be reasonably high tech and sophisticated. This paper describes just such a situation, where a large Cape Town based recycling and scrap metal facility makes use of a large industrial shredder to shred incoming scrap and separate and remove non-metallic components. This shredding plant basically consists of an in-feed conveyor, fed by a material handler that transports the scrap metal to a rotating disc rotor that employs hammers to shred the scrap material. This shredded scrap metal is then conveyed to a separation plant. The disc rotor of the shredder is powered by a 2.2 MW electric motor that turns the rotor at between 430 and 495 RPM and supplies a maximum torque of approximately 43.3 kNm. In order to accommodate the relative movement between the rotor of the shredder and the separately mounted electric motor, the torque is transmitted using a Cardan shaft.

This Cardan shaft with a 2.5 metre operating length consisted of two universal joints, with forged yokes, welded on to either end of a splined tubular shaft, Figure 1. After two years and four months in operation the shaft failed at the weld, labelled ‘F’ in Figure 1, joining the forged end of the spline to the tubular shaft.

The shaft was repaired shortly after being inspected and the fracture evidence, other than photographic, from the failed side of the shaft that was attached to the spline, was consequently destroyed. The one end of the tubular section of the shaft, was however cut off, and retained for further inspection and failure analysis, but this did imply that the tubular shaft section was now somewhat shorter.

Unfortunately this repaired Cardan shaft also developed fatigue cracking in an almost identical location, as this was discovered during a scheduled non destructive testing (NDT) inspection, using time of flight diffraction (TOFD) ultrasonic methods, two months after the first repair. The extent of fatigue crack growth, as inferred from this TOFD inspection, almost continuous circumferentially from the inside surface and up to 12 mm deep, implied that the Cardan shaft was in imminent danger of failing completely in no more than three weeks of further service. Consequently the shaft was ground clear in the weld at this fatigue crack location, and repaired a second time, this time with an improved weld procedure which included an 80° C pre-heat and a gas tungsten root run, as well as automated sub arc welding with enhanced filler wire.

Interestingly, during the repair and grinding out of the first weld repair, down to the spigot/tube junction, in preparing an 18mm deep and 25mm wide single “V” weld preparation, evidence of the fatigue crack became apparent. The fatigue crack was visually detected at a depth of ~5mm below the surface, and found to run for approximately 50mm circumferentially. At a depth of 8mm this crack was found to be continuous around the inner circumference of the shaft, which strongly vindicated the TOFD NDT report. Further grinding indicated, at 16mm below the surface, that there was a continuous lack of fusion defect, approximately 2-3mm deep right around the circumference, and that this had most probably caused the rapid initiation and propagation of this second crack.

In view of the original repair developing a second fatigue crack so rapidly, and also because of the shaft shortening, the shaft could not afford to be weld repaired again, a replacement Cardan shaft was ordered from the USA. Unfortunately the delivery time of this replacement was approximately six months, and both the short term and long term structural integrity of

the shaft was therefore a matter of concern. In order to manage the operation of the plant safely, it was appropriate to undertake a fracture mechanics based fatigue life prediction analysis of the newly repaired shaft. This paper concerns this very fracture mechanics fatigue life analysis, which makes significant use of reliable flaw size estimates obtained using ultrasonic TOFD measurements. It is appropriate firstly, however, to examine the characteristics of the original failure.

2. FAILURE ANALYSIS FINDINGS

2.1. Macroscopic Observations

The shaft had fractured at the weld joining the forged end of the spline to the tubular shaft breaking the shaft into two pieces approximately 770 and 1630 mm long, Figure 2 and Figure 3 respectively.

As depicted in Figure 2 and Figure 4, the shaft had failed in the region of the shoulder between the spigotted end of the male part of the spline. Figure 2 and Figure 4 also show that the fracture surfaces had suffered secondary mechanical damage as a result of the failure - probably caused by contact between the end of the shaft and the reinforcing ring that had been installed in the wall between the motor and the shredding plant. Clear so called 'clamshell' markings, characteristic evidence of fatigue, were evident on the fracture surfaces, Figure 4 and Figure 5. These 'clamshell' marks were orientated at approximately 45° degrees to the axis of the bearings in the yokes indicated by the dashed line in Figure 4.

While cutting the specimens for micro observation from the ring removed from the end of the shaft for inspection, it was noted that there was significant residual stress in the ring (the ring sprang apart approximately 2.5 and 6mm in the radial and circumferential directions respectively on final cutting). These stresses were not quantified, however, as the effects of the deformation caused after the final failure could not be assessed.

2.2. Micro observations

Further clear evidence of 'clamshell' markings was highlighted during the microscopic investigation, Figure 6 and Figure 7. Figure 6 furthermore shows the relatively greater degree of roughness of the outer regions of the fracture surface - which indicated that these outer regions were the areas of final fast fracture - which in turn implied that the crack initiated at the inner surface and propagated outward. The crack also propagated in the region of the interface of the weld heat affected zone (HAZ) and parent plate. This was further confirmed by areas indicative of the rapid failure of weld material near the outer regions of the fracture surfaces, Figure 8. These figures also show that the shaft had fatigued over the majority (between 70 and 90% depending on location) of the section thickness before final failure occurred. This indicates that both the cyclic and the mean stresses were low - but just high enough to cause fatigue in the presence of a stress concentrating feature.

Figure 7 also shows a region of discoloration at the inner surface of the shaft. It is believed that this discoloration was caused by the overheating of the shaft (due to friction)

in the period just after final failure prior to the hollow shaft disengaging from the spigot at the end of the splined section.

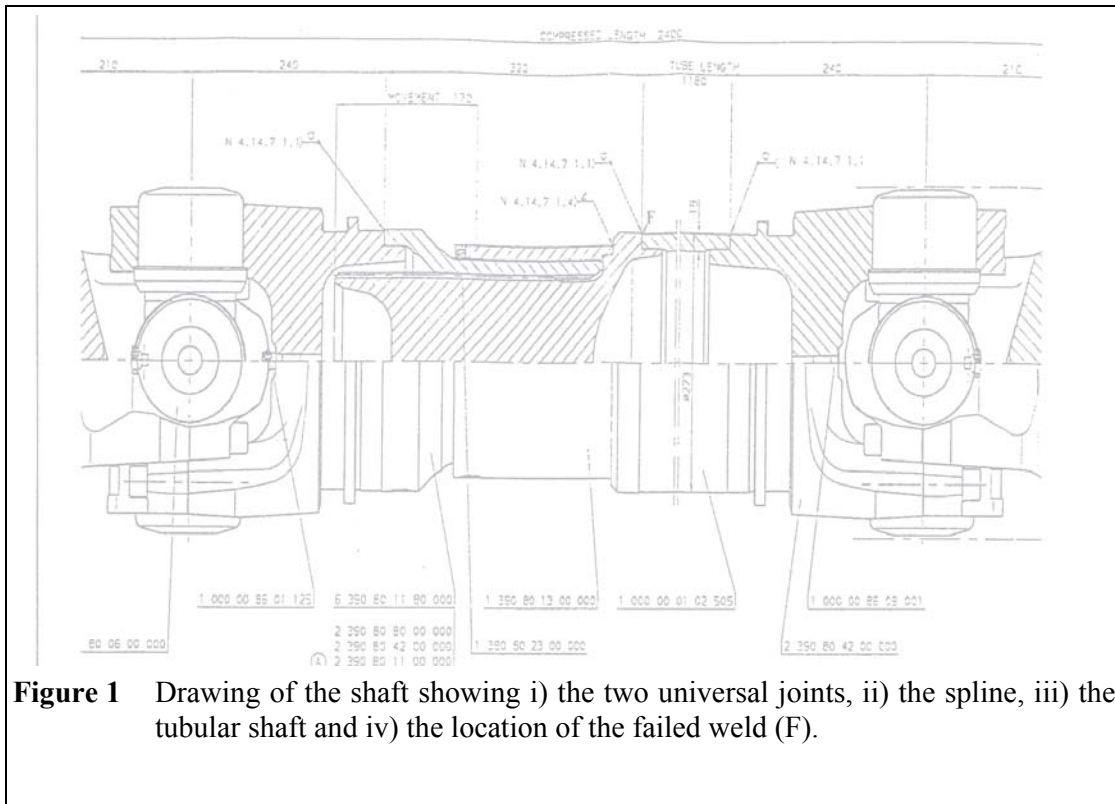


Figure 1 Drawing of the shaft showing i) the two universal joints, ii) the spline, iii) the tubular shaft and iv) the location of the failed weld (F).

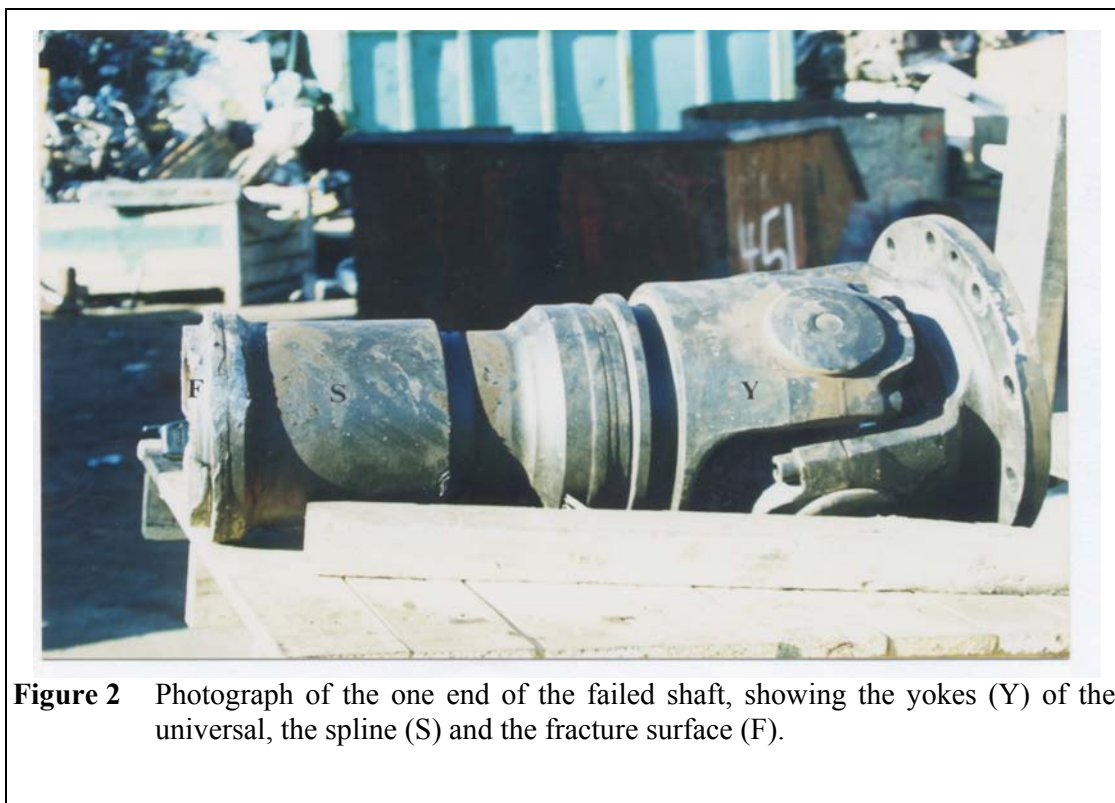


Figure 2 Photograph of the one end of the failed shaft, showing the yokes (Y) of the universal, the spline (S) and the fracture surface (F).



Figure 3 Photograph of the other end of the fractured shaft.

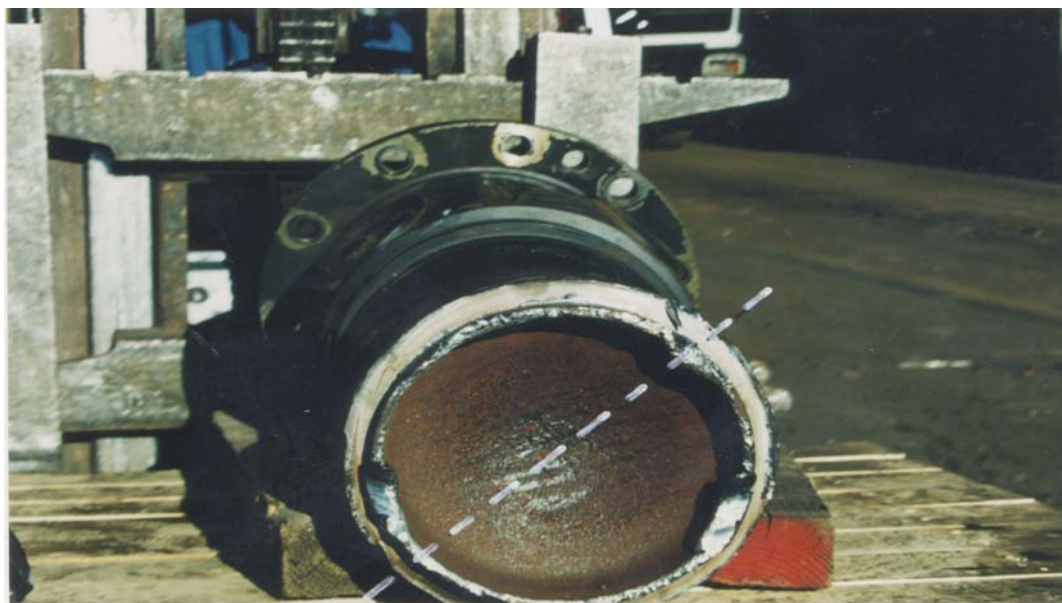


Figure 4 Photograph of the fracture surface of the end of the shaft shown in Figure 2. Evidence of so called 'clamshell' markings, characteristic evidence of fatigue, orientated at approximately 45° (when viewed from down the shaft) to the axis of the yoke (white dashed lines) are clear.



Figure 5 Close up photograph of the fracture surface of the end of the shaft shown in Figure 4. So called 'clamshell' markings and a variation of their orientation was clearly evident.



Figure 6 Micrograph (4.75x magnification) of the fracture surface of the end of the shaft shown in Figure 3 showing further evidence of 'clamshell' markings.



Figure 7 Micrograph (4.75x magnification) of the fracture surface of the end of the shaft shown in Figure 3 showing evidence of 'clamshell' markings in another region of the shaft. In comparison to those in Figure 6, a change in orientation of the 'clamshell' markings is clearly evident.



Figure 8 Micrograph (10x magnification) of the fracture surface of the end of the shaft shown in Figure 3 showing evidence of 'clamshell' markings as well as areas of fast fracture with an appearance consistent with that of fast fracture of dendritic crystalline weld material near the outer diameter of the shaft (right).

2.3. Material composition

In order to ascertain the material type a sample of the material and the weld was cut from the ring removed from the end of the fractured section of shaft shown in Figure 3. Analysis was conducted on both the weld material and parent plate. A summary of the percentage composition of the important elements for both the weld and parent plate material is contained in the following table. The composition of the parent plate is not unlike that of the steel manufactured to DIN StE 315 which is also shown in the table for comparison purposes. The exact steel specification for the material used to manufacture the Cardan shaft is not known, but it is likely, due to the similarities in the chemical composition of the two steels, that the material properties used for the Cardan shaft would have been similar to those of StE315 - namely i) a specified yield of 315 MPa, ii) an ultimate tensile stresses of between 440 - 560 MPa and iii) an ISO V notch toughness of 31 and 55 J in the transverse and longitudinal directions respectively.

It is of interest to note that the slightly increased values of Mn, Cr, and Mo in the weld would have tended to make the weld material harder and slightly more brittle¹.

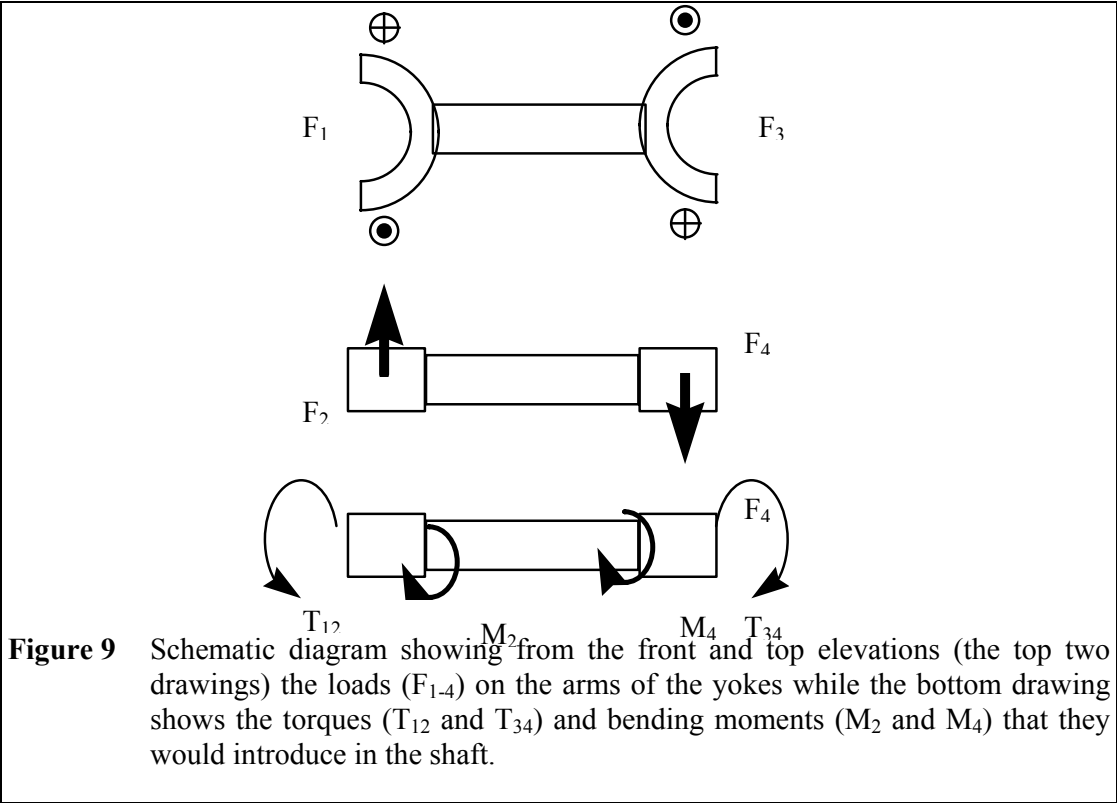
TABLE OF MATERIAL COMPOSITION TEST RESULTS								
	C %	Si %	Mn %	P %	S %	Cr %	Mo %	Nb+Ti +V%
StE 315 ¹	≤ 0.18	≤ 0.45	0.70- 1.50	≤ 0.035	≤ 0.030	≤ 0.30	≤ 0.08	≤ 0.05
Parent Plate	0.1666	0.2961	1.279	0.0107	0.0011	0.1197	0.0286	0.011
Weld Material	0.074	0.670	1.874	0.0208	0.081	0.797	0.3867	0.011

2.4. Stress analysis

The simple torsional load stress state in a Cardan shaft is complicated by a number of additional factors. One of these factors is caused by an intrinsic problem associated with universal joints of the type employed in this Cardan shaft - namely the variation of the angular velocity ratio between the driven and driving shaft^{2, 3}. That is, the angular velocity of rotation, and hence acceleration, of the driven (angled) shaft is not constant relative to that of the input shaft. The maximum acceleration of the driven shaft occurs when the yokes of the angled shaft have moved ~45° from the vertical position (when viewed down the shaft) and hence occurs twice per revolution. The effects of this varying angular velocity/acceleration at the output, are minimised when two universal joints are used and the angles of both the input and output shaft to the intermediate shaft are similar. However, even though there is little or no fluctuation of the angular velocity/acceleration (and hence the loading) of the output shaft, that of the intermediate shaft fluctuates at twice the rotational frequency.

An additional complexity is introduced by the bending moments introduced into the shaft through the arms of the yokes, M_2 and M_4 , Figure 9. These moments and their effects are most easily visualised using a ring or section of flexible tube, and loading it with the moments as illustrated in Figure 9 and Figure 10. These moments that act in the plane of curvature of the shaft. (i.e. opposite sides of the curved surface) and fluctuate at twice the rotational frequency due to the fluctuation of loads F_1 and F_2 . Under the influence of these moments the shaft tends to distort from its circular section into an oval one orientated $\sim 45^\circ$ to the axis of the yokes, Figure 10. This distortion therefore introduces additional fluctuating stresses which have a maximum at $\sim 45^\circ$ to the axis of the yokes, that fluctuate at twice the rotational frequency. As the moments also cause distortion, which takes the form of a ‘double S’, in and out of the plane of Figure 10, they would also have tended to induce a relative axial movement in the material of the shaft. Analysis of the magnitude of these stresses is complex and a full detailed analysis would have required finite element techniques which, although possible, was considered to be beyond the scope of this present investigation.

Although the preceding discussion gives background and understanding to the causes and variation of the stress state in the shaft, much may be gained by simply analysing the torsional stresses identified during the investigation initiated by GEC ALSTHOM⁴ (hereafter referred to as the GEC investigation). Torsional stresses for the varying load cases were analysed using simple elastic theory and were then employed in a fatigue life analysis as discussed in Section 2.5.



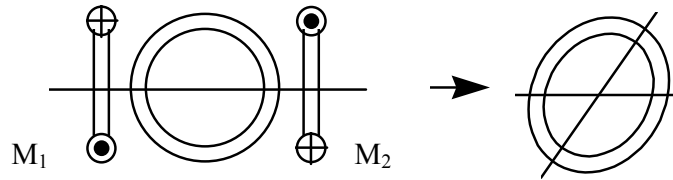


Figure 10 Schematic diagram illustrating the effect of the distortion, as seen from the axial elevation, caused by the bending moments M_1 and M_2 that would have been introduced into the shaft through the arms of the yoke.

2.5. Analysis of the loading conditions

The report concerning the GEC investigation of the loads produced in the shaft by the motor, showed that the shaft loading was predominantly of a pulsating nature. Comparison of the fatigue torque limit specified for the shaft⁵ and the measured torsional loads identified during the GEC investigation shows that the specified limit (142.8 kNm) for pulsating loads was approached but not exceeded by the so called ‘torque reversal’ (~135 kNm) load case. How representative the nature of this single load event recorded in the report is not stated and it must therefore be concluded that the specified pulsating limit was probably exceeded on occasion. This loading event is considered to occur approximately eight times per day (~4800 occurrences in the service life of this shaft) and is the only load case where torques exceeding 120 kNm were recorded.

2.6 Fatigue Life Prediction

It was not clear exactly how these fatigue torque limits⁵ were established from the limited data available, none the less it was possible to undertake a preliminary fatigue life estimate based on fracture mechanics methodologies. The approach here was to make use of conventional fracture mechanics principles where the propagation phase of the fatigue cracking can be characterised by the so called “Paris equation”, in which the crack growth rate, da/dN , and the cyclic stress intensity amplitude, ΔK , are related exponentially, i.e.

$$da/dN = C\Delta K^m$$

From a knowledge of the unique material parameters, C and m, that refer to the fatigue behaviour for the particular steel, as well as load spectrum and likely initial flaw sizes, it is possible to integrate the Paris equation between limits of initial flaw sizes and critical flaw size, to obtain the likely number of fatigue cycles to ultimate failure. This procedure was undertaken for various scenarios, including (a) the lifetime to the first failure (two years and four months); as well as (b) the lifetime to be expected after the second repair.

This analysis of the original fatigue life (a) (undertaken using a conservative summation approach) showed that with an appropriate, and very reasonable, stress concentration factor, failure of the shaft by fatigue mechanisms, solely under the influence of the torsional loads, was plausible and entirely consistent with the elapsed cyclic life actually experienced. This analysis was based on:

- The loading cases identified in the report on the investigation into the bearing loads of the electric motor initiated by GEC Alsthom.
- Assumed, but appropriate material property (fatigue Paris equation C and m) data⁶.
- A probable occurrence of these loads, in an attempt at a load spectrum, as identified by SA Metal⁷.
- Torsional stress calculated with a local stress concentration factor of 2.25 at the root of the weld.
- An assumed initial flaw size of 0.5mm.
- An appropriate Y compliance for an edge crack starting from a cylinder inner surface.

Although this analysis gives an indication that the torsional loads acting alone would have been sufficient to cause failure, it must be borne in mind that without measured material fatigue data and an accurate load frequency spectrum history, it is not possible to predict *precisely* when failure would occur. The analysis does, however, show that with entirely reasonable input parameters, fatigue to failure is not only quite plausible but highly likely.

With regard to the fatigue life prediction following the second repair, (item (b) above), while awaiting the delivery of the replacement Cardan shaft, the expected fatigue lifetime was of the order of four to five months, if the initial assumptions were correct. Since this predicted lifetime was based on a conservative fracture mechanics analysis, and was less than the delivery time for the replacement shaft, it was in order that the repaired shaft be non destructively inspected with a highly accurate NDT system, to see if there was indeed any fatigue crack growth. Consequently ultrasonic TOFD NDT was selected since TOFD has a sizing error of approximately $\pm 0.5\text{mm}$ in the laboratory and even $\pm 1.0\text{mm}$ in the field, which was quite acceptable for the current inspection application.

TOFD NDT inspection tests were undertaken soon after the repair in March and then as scheduled in mid July and again in October 2000. Four flaw regions were recognised and characterised (LW1 A,B,C,D) and their evolution is summarised in the Table. Comparison of the results shows that all the indications in LW1 (except those for LW1A) were larger at the time of the October inspection. If this increase was indeed “growth”, then the flaws in the region have grown by $\sim 1.5\text{mm}$ and a flaw/indication of 5.6mm had appeared at LW1C in a period of 12 weeks.

Description	Flaw size (mm) (19 July 2000)	Flaw size (mm) (11 Oct 2000)	Change in size (mm) (12 week)
LW1A	4	4	0
LW1B	3	4.5	1.5
LW1C	None detected	5.6	5.6
LW1D	None detected	3.3	3.3

Assuming the change in flaw size was indeed “growth”, then it was believed that the shaft was likely to fail during the ten week period between the last inspection and the expected date of replacement, approximately during the last week of the year. On the other hand if the flaws in LW1C and LW1D were (i) pre-existing, and simply not detected during the earlier inspection, or (ii) not growing, then the situation was somewhat less serious.

On this TOFD evidence, a further inspection was undertaken which indicated small but acceptable further growth. The inspections also served to “benchmark” the fatigue crack growth and life predictions more precisely, with minor adjustment to the C values so that there was strong correlation between the actual amount of measured crack growth and the life prediction crack growth. This process then refined subsequent fatigue life prediction and provided increased confidence in the methodology.

Furthermore analyses of this sort, specifically in variable load situations, may be used as a ‘sensitivity analysis tool’ to identify specifically detrimental load cases. Removal of individual load conditions from the analysis indicated that the load cases identified in the GEC report as ‘heavy loading’ and ‘torque reversal’ were the most significant contributors to the failure. Although the ‘torque reversal’ load case forced the shaft to carry the highest torsional loads, the analysis showed that the high frequency of occurrence (ie large number) associated with the ‘heavy load’ load case, acting in conjunction with its associated moderately high loads, was the single most significant contributor to the failure.

3. DISCUSSION AND CONCLUDING REMARKS

It is clear from the fracture evidence that the original shaft failed by fatigue mechanisms and that the stress levels in the shaft causing the fatigue failure were relatively low - well within the static design capabilities of the shaft. The fracture evidence furthermore shows that the failure initiated at the inner surface of the shaft, in the HAZ/parent plate interface of the weld affixing one of the forged ends to the intermediate shaft, and propagated outwards.

Analysis of the material composition test results showed nothing untoward, and no gross material micro-structural defects were noted.

The ~45° orientation of the fatigue initiation points, as manifested by the clamshell markings, shows that the failure was probably influenced to some extent by the moments introduced in the shaft through the arms of the yoke. The stresses associated with these moments were not rigorously analysed (using finite elements, for example), however, a preliminary analysis of crack growth and fatigue life showed that failure by fatigue mechanisms was entirely plausible under the sole action of the torsional load cases identified in the GEC report, and

sufficient to cause the original failure. Although the highest loads, that were in the region of the specified torque limits of the shaft, were associated with the 'torque reversal' load case identified in the GEC investigation, the stresses associated with the 'heavy load' load case were identified as the most detrimental, because of their greater number.

The fracture mechanics based fatigue life prediction methodology, combined with an accurate NDT flaw sizing capability, TOFD in this case, has enabled intelligent NDT inspection intervals to be determined and any fatigue crack development monitored. All that is required for such an analysis are material fatigue characteristics, (C and m, together with fracture toughness), accurate indications of initial flaw sizes and some confidence in the cyclic loading spectrum the component experiences. With such input data, reliable estimations of expected life, or alternatively degree of crack growth in a certain interval, are relatively straightforward. In this way catastrophic failure was avoided and the repaired Cardan shaft ran successfully until its replacement arrived, in early January 2001.

It was also of great interest in this paper to see the close correlation of these TOFD measured flaw sizes, prior to the second repair, with the actual flaw sizes, as revealed when the weld was ground out.

This paper illustrates the synergistic benefits of using high technology NDT (TOFD in this case) with fracture mechanics based fatigue life prediction. The marriage of these two technical disciplines provides a quantitative methodology for assessing safe plant operation, as well as a new philosophy of "living with defects", while still ensuring that the system is fully operational and "fit for purpose".

REFERENCES

-
- ¹ 'Stahl Schlüssel', 1989, pp 72-74.
 - ² VM Faires and RM Keown, *Mechanism*, McGraw Hill, 1939, pp 303 - 306.
 - ³ J Morrison and B Crossland, *Introduction to Mechanics of Machines*, Longmans, 1969, pp 119-122.
 - ⁴ M Newby of the ESKOM Technology Group, *Report on the findings of an investigation initiated by GEC ALSTHOM (South Africa) titled 'Torque and Vibrational Analysis on a Metal Shredder Motor'*, Report No: 7753S5091, May 1998, pp 1-34.
 - ⁵ Facsimile communication from D. Koopman, SA Metal, to C Emslie and J. Press, CRS, 6 March 2000.
 - ⁶ British Standards code BS PB 6493 1991, *'Guidance on methods for assessing the acceptability of flaws in fusion welded structures'*.
 - ⁷ Facsimile communication from D. Koopman, SA Metal, to J. Press, CRS, 18 March 2000.